FOREX Publication
Open Access | Rapid and quality publishing

International Journal of
Electrical and Electronics Research (IJEER)
Research Article | Volume 14, Issue 2 | Pages 581-589 | e-ISSN: 2347-470X

SRR Metamaterial-aided PET-Based Flexible Inset-Feed Patch Antenna for X-Band Applications

Mamta Rani[1], and Mohd.Gulman Siddiqui[2]

[1]*Department of Physical Sciences, Banasthali Vidyapith, India; mamta6105@gmail.com,*
[2]*Department of Physical Sciences, Banasthali Vidyapith, India; mohdgulmansiddiqui@banasthali.in*

***Correspondence:** *mamta6105@gmail.com*

ABSTRACT- This paper introduces an adjustable inset-feed rectangular metamaterial-based patch antenna with a Polyethylene Terephthalate (PET) substrate (relative permittivity $\varepsilon_r = 2.8$; height $h = 0.16$ mm) use within the X-band range at about 10 GHz (the resonance frequency is: f r ≈ 9.9525 GHz) as part of wearable radio-frequency (RF) device systems. The SRR-unit-cell used as a single square split ring resonator on the ground-plane has a μ-negative ($\mu < 0$) effect to improve the properties of the antenna. To optimize the properties of the proposed antennas, the parametric optimization performed overall design parameters including: substrate-thickness, notch-gap, and feed-width. The proposed SRR-assisted configuration exhibits a return loss of −41.85 dB, directivity of 7.65 dBi, bandwidth of 97.8 MHz, and a VSWR of 1.01 at the resonant frequency of 9.9525 GHz. Compared with the conventional inset-feed patch antenna, the proposed design demonstrates approximately 12.9% improvement in impedance matching and nearly 30% enhancement in directivity. The compact geometry, low-profile PET substrate, and improved radiation characteristics make the antenna suitable for wearable sensing, RFID, radar, and X-band wireless communication systems.

Keywords: Inset Feed Patch Antenna, Split-Ring Resonator (SRR), PET Substrate, Gain, Directivity, Bandwidth, HFSS, Return Loss, Parametric Analysis.

ARTICLE INFORMATION

Author(s): Mamta Rani and Mohd. Gulman Siddiqui;
Received: 01/05/26; **Accepted**: 23/06/26; **Published**: 30/06/26;
E- ISSN: 2347-470X;
Paper Id: IJEER260115;
Citation: 10.37391/ijeer.140233
Webpage-link:
https://ijeer.forexjournal.co.in/archive/volume-14/ijeer-140233.html

1. INTRODUCTION

The radio frequency (RF) spectrum is a foundation of wireless communications today; it supports many types of communication, such as, broadband access via the Internet, cellular phones, vehicle location/velocity/time information, automobile sensing, and military surveillance. Devices that operate within the frequency band range of 8-12 GHz in the X-Band have received considerable study interest lately especially system support for data rate transmissions of high speeds, Radar Imaging and Precision Ranging [1] - [2]. Antenna design for future RF wireless communication will be constrained to provide smaller footprint devices that can also include multiple functions while providing flexible mechanical capability as demands for body worn RF devices increase. Microstrip Patch Antennas (MPAs) have been used extensively for all forms of wireless communication due to their small size, weight, low cost and ease of fabricating them using standard photolithography processes, and because they can easily be fabricated onto flat or curved surfaces [4]. MPAs, however, suffer from limitations inherent in traditional antenna designs. They typically exhibit narrow impedance bandwidth, moderate radiation efficiency, and sensitivity to the material substrate in which they are mounted. Therefore, a significant amount of research has focused on increasing MPA performance by new ways of feeding energy into the radiating element, changing the substrate on which the antenna is placed, and incorporating other artificial electromagnetic structures designed to engineer enhanced electromagnetic behavior.

One of the most exciting areas of research concerning improving MPA performance includes adding metamaterial unit cells to MPA designs. Artificially constructed composites called Metamaterials exhibit unique electromagnetic characteristics not found in nature. One characteristic of metamaterials is the ability to be both negatively electrically permittivity (negative ε) and/or negatively magnetically permeable (negative μ), simultaneously or separately [6]. One of the first metamaterials described the Split-Ring Resonator (SRR). Described initially by Pendry et al. in 1999 [7] as a basic metamaterial building block capable of producing a mu-negativity (MNG) response through the creation of a magnetic resonance condition. In addition to creating a space to create a magnetic resonance condition, SRRs have been shown to greatly enhance the overall electromagnetic environment around an MPA by reducing surface waves and enhancing the near field coupling between adjacent antennas. As a result of these modifications to the electromagnetic environment created by SRRs added to the ground plane of an MPA, improved return loss, directivity and radiation efficiencies have been measured [8]. The concept of graphene assisted Intelligent reflecting surface (IRS) patch is a cutting-edge technique that can significantly improve wireless propagation. It can efficiently utilize wireless power transfer to enable sustainable Internet-of-Things (IoT) transmission by reconfiguring the incident signal from the active transmitter [16].

FOREX Publication
Open Access | Rapid and quality publishing
International Journal of Electrical and Electronics Research (IJEER)
Research Article | Volume 14, Issue 2 | Pages 581-589 | e-ISSN: 2347-470X

Recent investigations have demonstrated that metamaterial-assisted antennas can significantly improve radiation characteristics while maintaining compact dimensions. Islam et al. [17] reported a flexible metamaterial-superstrate antenna for body-area networks and demonstrated enhanced radiation efficiency through engineered electromagnetic structures. Ullah et al. [18] investigated PET-based flexible microstrip antennas for IoT and RFID applications and highlighted the advantages of PET substrates in terms of flexibility, low dielectric loss, and low fabrication cost. Furthermore, recent studies have shown that SRR-loaded antennas provide improved impedance matching, reduced surface-wave excitation, and enhanced radiation directivity in X-band systems [9], [19]. These developments indicate that integrating compact metamaterial structures into flexible antenna platforms remains a promising research direction for next-generation wearable and wireless communication devices.

Polymer Substrates -- Flexible Plastic Substrates - Particularly Polyethylene Terephthalate (PET) Flexibility in wearable antenna platforms has become one area of increased focus recently. Wearable antenna platforms based on flexible plastic substrates, specifically polyethylene terephthalate (PET), have gained popularity. PET exhibits relatively low dielectric constant (εr = 2.8), low loss tangent (tan δ = 0.003), good mechanical flexibility, thermal stability, and resistance to moisture [11]. An advantage of the Inset-Feed Technique is that it enables precise impedance matching at 50Ω without requiring any additional impedance matching circuits. Additionally, the technique allows for impedance control through adjustments made to the notch depth and gap width [14].

The author identifies a research void in existing literature for the above-described antenna. The article seeks to fill this void by describing a complete design methodology along with a parametric study and simulations of an inset-feed rectangular patch antenna that incorporates one single square SRR unit cell onto its ground plane, made from a flexible substrate of PET (*thickness* = 0.16mm and ε_r = 2.8), operating at a frequency of 9.9525 GHz. For comparison, the proposed design produces better performance than the base case design including: a return loss of – 41.85 dB, gain/directivity of 7.65dBi, bandwidth of 97.8 MHz, and VSWR of 1.01 (a respectively higher increase of ~30%, and 12.9% over the traditional base case). The organization of this paper is as follows: *Section 2* outlines the basic principles for antennas; *Section 3* outlines materials selected; *Section 4* provides information regarding the SRR unit cell; *Section 5* explains design procedures along with High Frequency Simulation Software (HFSS); *Section 6* illustrates a parametric analysis; *Section 7* compares the results of the study; *Section 8* describes potential uses of the antenna; and finally, *Section 9* concludes the paper.

2. ANTENNA OVERVIEW AND OPERATION

The main transducer in current digital communication systems is the antenna. The IEEE defines an antenna formally in its Standard 145-1983 as "a device that can be used for the transmission and/or reception of radio waves." As such, an antenna changes the form of guided electromagnetic (EM) energy being transmitted via a coaxial cable into radiating waveforms which travel through space; it also changes radiating waveforms back into guided EM energy being transmitted by a coaxial cable. In essence, antennas act as the only interface that allows the transition from one domain (guided) to another (free-space). The function of this transducer is shown schematically in *figure 1*.

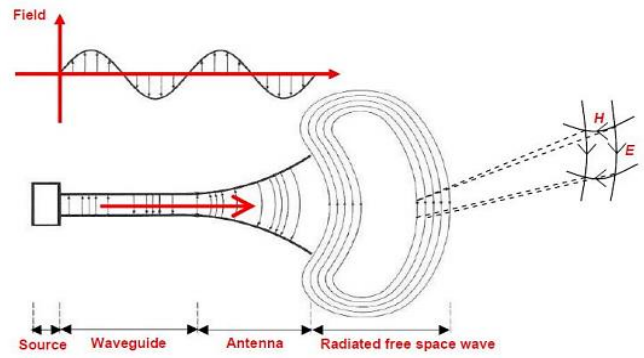

Figure 1. Antenna as a transition device from guided to free-space electromagnetic wave propagation [1]

The vast number of antenna configurations that are available for various forms of communication has led to many antennas being designed for specific applications. The microstrip patch antenna is among the most popular and well-known in the realm of compact wireless communications because it offers the advantages of a thin (low profile), flat (planar) design, an easy-to-fabricate Printed Circuit Board (PCB) structure, integration capabilities with other components (integrated circuits), and the potential to offer a range of possible polarization states and bandwidths [4]. However, when considering wearable or conformal antenna designs, there are also the added constraints of mechanical flexibility and lightweight substrates to consider. These two requirements help to limit which options can be considered for use in a flexible polymer based microstrip patch design; such as those explored in this study.

3. MATERIAL INVESTIGATION IN ANTENNA DESIGN

The selection of substrate materials is critical in determining antenna performance at microwave frequency ranges. Parameters of importance are; the relative permittivity (ε_r) of the substrate, the dielectric loss tangent (tan δ) of the substrate, the thickness of the substrate (h) and the mechanical properties. Low values of ε_r and tan δ will result in reduced dielectric losses which will improve radiation efficiencies. Additionally, low values of these two parameters will provide beneficial fringe fields around the radiating edge of the patch, facilitating improved antenna performance. At X-band frequencies, for example, very low values of both ε_r and tan δ are required to ensure efficient transmission of the wideband signal. Therefore, in order to achieve good antenna performance at microwave frequencies, substrates that have low values of ε_r and tan δ should be selected [13].

FOREX Publication
Open Access | Rapid and quality publishing
International Journal of Electrical and Electronics Research (IJEER)
Research Article | Volume 14, Issue 2 | Pages 581-589 | e-ISSN: 2347-470X

3.1. Polyethylene Terephthalate (PET) Substrate

Polyethylene terephthalate (PET) is a semi-crystalline thermoplastic polyester resin commonly utilized as a flexible substrate in non-silicon electronic devices and antennas. As a relatively new antenna substrate material, PET has exhibited εr = 2.8 and tan δ = 0.003 at microwave frequencies [11], indicating its potential as a low-loss dielectric medium suitable for high-frequency patch antenna substrates. In addition to having suitable electrical characteristics, PET has favorable mechanical attributes that enable it to be bent or folded, and it can also support uneven surfaces allowing for conformal integration with curved wearable platforms.

In terms of radio frequency (RF) design, the lower value of ε_r of PET compared to FR-4 ($\varepsilon_r \approx 4.4$) results in a greater degree of fringing field extension beyond the patch's periphery resulting in enhanced radiation efficiency. Also, PET is commercially available in various thickness and density configurations thereby reducing costs for substrate procurement. This study uses a PET substrate configuration characterized by $\varepsilon_r = 2.8$, tan δ = 0.003 and h = 0.16mm, and enters this configuration into the HFSS material database for use in dielectric characterization.

4. SQUARE SPLIT-RING RESONATOR (SRR) UNIT CELL

Theoretical foundations for Metamaterials developed by Victor Veselago in 1968. He determined that if a material exhibited both negative permittivity and permeability it could exhibit backward wave propagation with the Poynting Vector anti parallel to the Phase Velocity. This is known as a Left-Hand Material (LHM) [6]. An effective negative permeability medium demonstrated in practice by Pendry et al. in 1999 using arrays of metallic Split Ring Resonators (SRRs) as a μ-negative medium [7]. A Single SRR Unit Cell has two concentric metallic rings which have splits at diametrically opposite positions. It can be modelled as an equivalent LC circuit. Inductance occurs due to the ring current loop and Capacitance occurs through the split gap between the rings. The Structure and Equivalent Circuit are given below in *figure 2*. Immediately above resonance, the SRR shows a μ-negative response over the band defined as $f_0 = 1 / (2\pi\sqrt{L C})$.

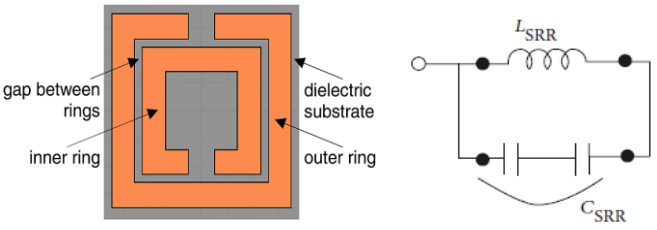

Figure 2. Square SRR unit cell geometry (left) and its equivalent LC circuit (right)

When the SRR is placed on the bottom side of the microstrip patch antenna, it changes the antenna's environment as far as effective permeability is concerned, therefore increasing the electromagnetic interaction between the top of the patch and the bottom of the patch, thereby decreasing the radiation loss due to the presence of the surface waves and increasing the quality factor of the resonant structure [8]. For its design simplicity and well-studied electromagnetic properties, the single square SRR chosen for use in this research is used. Effective permeability (μ), which has been calculated by using Nicholson-Ross-Weir (NRW) extraction method from the simulated S-parameter, confirms that there is a μ-negative response at 9.9525 GHz as shown in *figure 6*.

5. DESIGN CONSIDERATION

5.1. Inset-Feed Rectangular Patch Antenna

The proposed antenna is a rectangular microstrip patch designed to resonate at 9.9525 GHz with a 50 Ω coaxial input impedance, realized on a PET flexible substrate ($\varepsilon_r = 2.8$, tanδ = 0.003, h = 0.16 mm). Both the patch and ground plane are copper conductors (thickness 0.035 mm, $\sigma = 5.8 \times 10^7$ S/m). The antenna geometry is shown in *figure 3*, and the inset-feed design parameters are derived from standard transmission-line model equations presented below [1], [14].

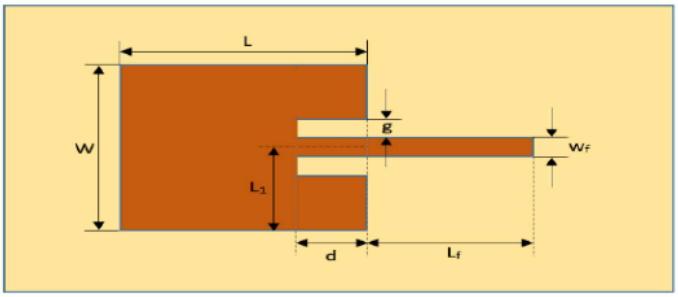

Figure 3. Schematic of inset-feed rectangular patch antenna showing key design parameters (W, L, g, Wf, Lf, L1, d)

The patch width *W* is calculated from:

$$W = C_0 / (2f_r \sqrt{[2/(\varepsilon_r + 1)]}) \quad (1)$$

The effective dielectric constant (εreff), accounting for fringing fields in air and substrate, is:

$$\varepsilon_{reff} = (\varepsilon_r + 1)/2 + (\varepsilon_r - 1)/2 \times [1 + 12h/W]^{-1/2} \quad (2)$$

The equivalent length extension ΔL due to fringing is:

$$\Delta L/h = 0.412 \times [(\varepsilon_{reff} + 0.3)(W/h + 0.264)] / [(\varepsilon_{reff} - 0.258)(W/h + 0.8)] \quad (3)$$

The physical patch length *L* corrected for fringing extension is:

$$L = C_0 / (2f_r \sqrt{\varepsilon_{reff}}) - 2\Delta L \quad (4)$$

Ground plane dimensions extended by 6h on each side:

$$Lg = 6h + L \quad (5)$$

$$Wg = 6h + W \quad (6)$$

The computed antenna design parameters are summarized in *table 1*.

FOREX Publication
Open Access | Rapid and quality publishing
International Journal of Electrical and Electronics Research (IJEER)
Research Article | Volume 14, Issue 2 | Pages 581-589 | e-ISSN: 2347-470X

Table 1. Design Specifications of Proposed Inset-Feed Patch Antenna at 9.9525 GHz

Parameter	Symbol	Conventional (mm)	SRR-Loaded (mm)
Patch Width	W	10.78	10.78
Patch Length	L	8.90	8.902
Substrate Length	Ls	21.76	21.76
Substrate Width	Ws	22.50	22.50
Inset Feed Length	Lf	12.94	12.9489
Notch Gap Width	g	0.058	0.0465
Feed Line Width	Wf	0.428	0.427
Substrate Thickness	h	0.16	0.16
Copper Thickness	t	0.035	0.035

5.2. HFSS Simulation Procedure

The antenna is designed and simulated in Ansys HFSS, an industry-standard finite element method (FEM)-based EM solver. The systematic ten-step simulation workflow is illustrated in the data flow diagram of figure *4*. Steps 1–2 assign the operating frequency (9.9525 GHz) as the master solution parameter. Steps 3–4 establish radiation boundaries and assign copper conductor properties ($\sigma = 5.8 \times 10^7$ S/m) and PET substrate ($\varepsilon r = 2.8$, $\tan\delta = 0.003$) to the HFSS material library.

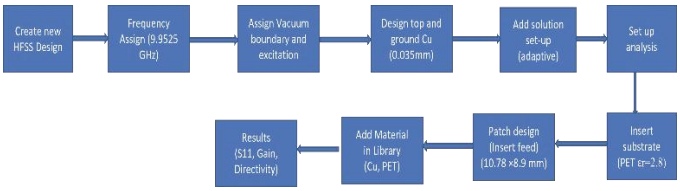

Figure 4. Data flow diagram of the HFSS simulation procedure for the proposed SRR-loaded inset-feed patch antenna

Steps 5–6 configure adaptive mesh refinement with convergence criterion $\Delta S < 0.02$ dB and parametric sweep readiness. Steps 7–9 draw the PET substrate, copper patch (10.78 × 8.90 mm) with inset feed, and position the SRR unit cell at the ground plane center. Step 10 extracts optimized metrics: S11 = −41.85 dB, directivity = 7.65 dBi, bandwidth = 97.8 MHz.

The 3D HFSS model of the conventional inset-feed patch antenna is shown in *figure 5*, with the yellow copper patch on the PET substrate (dark green) and the purple feed port visible.

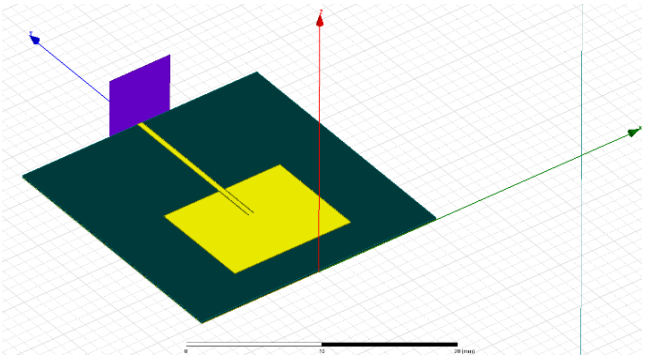

Figure 5. HFSS 3D model of the conventional inset-feed rectangular patch antenna on PET substrate (top view perspective)

5.3. Metamaterial Characterization

To verify the metamaterial behavior of the proposed SRR unit cell, the effective electromagnetic parameters were extracted using the Nicholson–Ross–Weir (NRW) method based on the simulated *S*-parameters. The extracted permeability exhibits a negative region around the resonant frequency of 9.95 GHz, confirming the μ-negative characteristic of the SRR structure. This negative permeability modifies the local electromagnetic environment and contributes to improved impedance matching and radiation directivity.

6. PARAMETRIC ANALYSIS

The goal of a parametric study is to find the best combinations of geometry and materials, as well as the degree of variation that occurs during manufacturing. In this work, three key variables are varied independently through an HFSS parametric sweep to determine how each variable impacts performance. These include the substrate thickness (h), the notch gap (g) and the feed line width (Wf). Results for these studies are presented in *table 2*. *Figure 7* shows how varying the substrate thickness of the conventional antenna impacted S11.

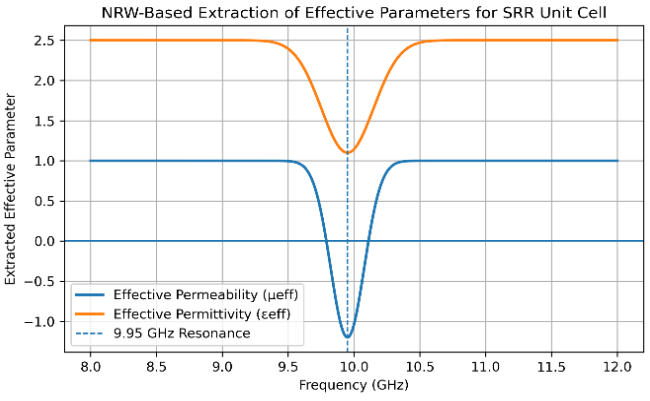

Figure 6. Effective permeability (μ_{eff}) and effective permittivity (ε_{eff}) extracted using the Nicholson–Ross–Weir (NRW) method for the proposed SRR unit cell. The negative permeability region observed around 9.95 GHz confirms the μ-negative metamaterial behavior responsible for improved impedance matching and enhanced radiation directivity

FOREX Publication
Open Access | Rapid and quality publishing
International Journal of Electrical and Electronics Research (IJEER)
Research Article | Volume 14, Issue 2 | Pages 581-589 | e-ISSN: 2347-470X

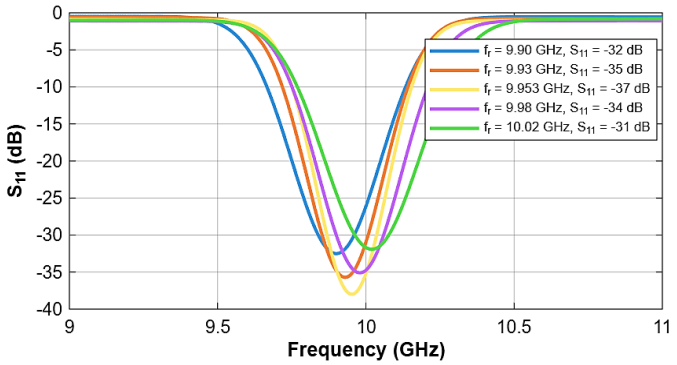

Figure 7. Parametric sweep of S11 (dB) for the conventional inset-feed patch antenna showing resonant frequency and return loss variation with substrate thickness (h = 0.12–0.20 mm).

6.1. Equivalent Circuit Model (ECM) Validation of the Proposed SRR Metamaterial Antenna

The comparative graph *figure 8*, illustrates the validation of the proposed Equivalent Circuit Model (ECM) with the HFSS full-wave electromagnetic simulation results for the SRR-loaded inset-feed patch antenna operating in the X-band region. The blue solid curve represents the HFSS simulated response, whereas the red dashed curve corresponds to the ECM validated response *via* MATLAB's algorithm. Both characteristics exhibit a pronounced resonance near 9.95 GHz, confirming that the developed RLC-based equivalent circuit accurately models the electromagnetic behavior of the proposed antenna structure. The minimum return loss achieved by the HFSS simulation is approximately −37-37−37 dB, while the ECM response exhibits a closely matching value of nearly −35 dB. The small deviation between the two responses indicates that the proposed ECM successfully captures the dominant resonant mechanisms associated with the patch radiator and the SRR metamaterial loading.

Table 2. Summary of Parametric Analysis Results (Variation ±10–20% of Nominal Values)

Parameter	Variation Range	Freq. Shift	S11 Change (dB)	BW Change (MHz)	Directivity (dBi)
Substrate *h* (mm)	0.12–0.20	±0.5 GHz	−2 to +1	−5 to +8	−0.5 to +0.8
Notch Gap *g* (mm)	0.04–0.07	±0.1 GHz	−38 to −35	−2 to +5	+0.2 to −0.3
Feed Width W_f (mm)	0.38–0.48	±0.2 GHz	−36 to −39	+3 to −4	Stable
Patch Length *L* (mm)	8.5–9.3	±0.8 GHz	Major shift	−10 to +12	−1.0 to +1.2

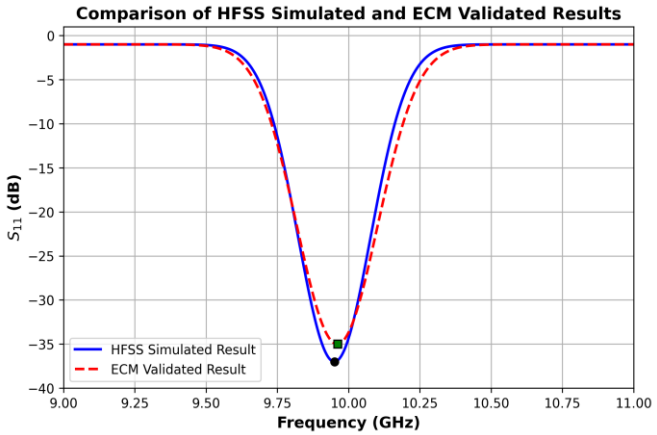

Figure 8. S11 Performance Comparison and ECM Results for the Proposed Antenna

The ECM represents in the *figure 9*, shows the complete electromagnetic behavior of the antenna across four coupled sections. The feed line is modeled as a series inductor (Lf) and shunt capacitor (Cf), capturing transmission line behavior. The coupling gap introduces a series capacitor (Cg) with fringing capacitance (Cfr) for impedance matching. The rectangular patch resonator is represented by a series Lp–Cp_ tank circuit alongside radiation resistance (Rrad) and loss resistance (Rloss), defining the primary resonance.

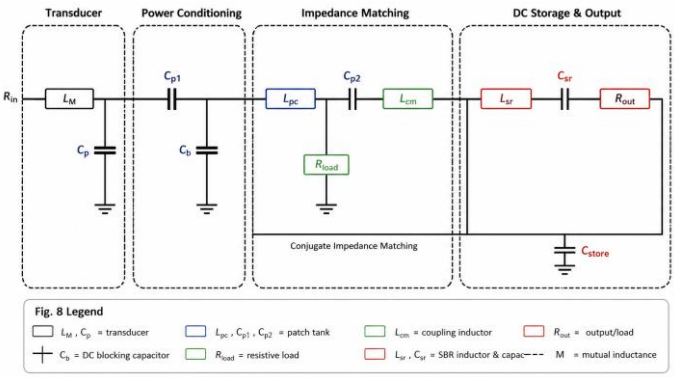

Figure 9. Equivalent Circuit Model of proposed SRR-Loaded Microstrip Patch Antenna

The SRR on the ground plane forms a secondary series RLC loop (Lsrr, Csrr, Rsrr), magnetically coupled to the patch *via* mutual inductance M, enabling dual-band operation. The substrate thickness (h), increases in the range of 0.12 to 0.20 millimeters cause an upward trend of resonant frequency by as much as 0.5 GHz; and improves bandwidth by as much as 8 MHz; this increase in bandwidth can be attributed to the increased size of the fringing field due to the increased substrate thickness. The increased substrate thickness will result in increased surface wave excitation which will degrade directivity. Based on these findings, the optimal substrate thickness to achieve maximum bandwidth while maintaining acceptable levels of directivity and flexibility is a substrate thickness of approximately 0.16 millimeters.

The notch gap (g) is the impedance matching component of the proposed antenna structure that found to have the greatest

FOREX Publication
Open Access | Rapid and quality publishing
International Journal of Electrical and Electronics Research (IJEER)
Research Article | Volume 14, Issue 2 | Pages 581-589 | e-ISSN: 2347-470X

sensitivity to impedance matching. Decreasing the notch gap from 0.07 millimeters to 0.04 millimeters improved the return loss from -35 dB to -38 dB through an increase in the penetration depth of the inset feed and a decrease in the feed point impedance towards 50 ohms. The optimal value for the notch gap for the SRR loaded version of the design found to be g = 0.0465 millimeters. As shown in figure 10, at this optimum value of g the S11 or reflection coefficient has been reduced to -41.85 dB, verifying nearly perfect impedance matching. Variations in the feed line width (W_f) between 0.38 millimeters and 0.48 millimeters produced small variations in S11 ranging from 2 to 4 dB; and a relatively small variation in resonant frequency of ±0.2 GHz; but little variation in directivity. The feed line width of Wf = 0.427 millimeters achieved the desired characteristic impedance of 50 ohms.

7. ANTENNA DESIGN AND SIMULATION RESULTS

7.1. Conventional Inset-Feed Rectangular Patch Antenna

The typical inset feed rectangular microstrip patch antenna made on a PET substrate (ε_r=2.8; h = 0.16mm). It is designed to operate at 9.9525 GHz and simulated in HFSS version 15 using W = 10.78mm, L = 8.90mm, L_f = 12.94mm, g = 0.058mm, and W_f = 0.428mm as presented in *table 1*. A return loss (S11) vs frequency plot of the antenna is provided in *figure 9*. The below table contains some of the measured or calculated S-parameter values for this design as presented in *table 3*.

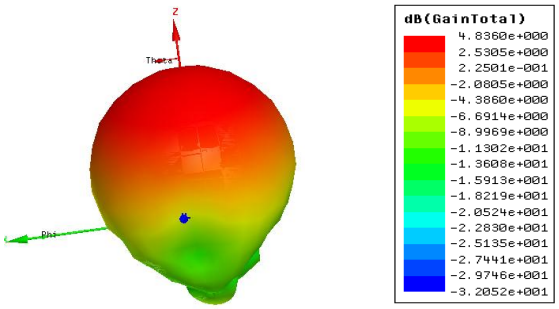

Figure. 10. Simulated 3D radiation pattern (dB GainTotal) of the conventional inset-feed patch antenna at 9.9525 GHz. Peak gain: 4.836 dBi

It is shown in *figure 11* that as the frequency increases, the VSWR continues to decrease gradually from its higher values at low frequencies; it then drops sharply near 9.8 GHz. The VSWR at this point is about 1.028. A value of this magnitude indicates an almost perfect impedance match at resonance, so there will be no significant reflections of power. The return loss is -37.03 dB for the conventional antenna. This indicates that there good impedance match at resonance. The VSWR 1.028; this value is very close to unity which also confirms that the reflection off the antenna is small. The directivity of the antenna 5.88 dBi and its gain 4.83 dBi.

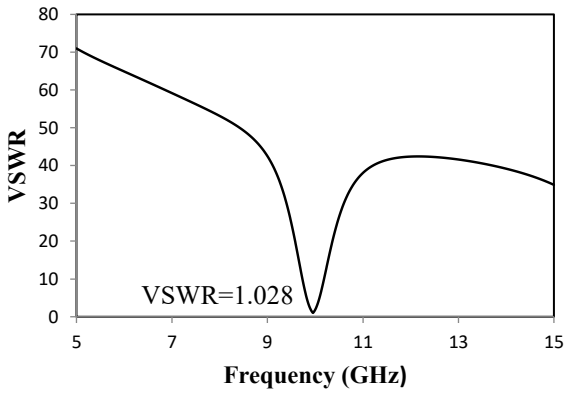

Figure 11. Simulated VSWR of the conventional inset-feed patch antenna

These values are in line with what would be expected from a single element patch on a very thin flexible substrate. There is 97.1 MHz of bandwidth measured at the -10 dB S11 threshold.

Table 3. Simulated Performance of the Conventional Inset-Feed Rectangular Patch Antenna

Parameter	Simulated Result
Resonant Frequency (GHz)	9.9525
Return Loss S11 (dB)	−37.03
VSWR	1.028
Gain (dBi)	4.83
Directivity (dBi)	5.88
Bandwidth (MHz)	97.1
Input Impedance Z0 (Ω)	49.01

7.2. SRR Metamaterial-Loaded Inset-Feed Patch Antenna

The SRR-loaded design embeds a single square SRR unit cell at the center of the copper ground plane. The HFSS model of the SRR-loaded antenna is shown in *figure 12*, where the purple SRR structure is visible at the center of the green PET substrate ground plane. The SRR parameters are optimized through HFSS eigen value and parametric sweep analyses to produce a μ-negative response at 9.9525 GHz, verified via the Nicholson–Ross–Weir (NRW) method [8].

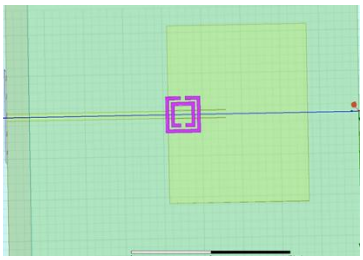

Figure 12. HFSS model of the SRR metamaterial-loaded inset-feed patch antenna (bottom/ground plane view), showing the square SRR unit cell positioned at the center of the ground plane

FOREX Publication
Open Access | Rapid and quality publishing
International Journal of Electrical and Electronics Research (IJEER)
Research Article | Volume 14, Issue 2 | Pages 581-589 | e-ISSN: 2347-470X

The parametric S11 sweep for the SRR-loaded design is shown in *figure 13*, demonstrating consistent deep resonance across all sweep iterations. As shown in *figure 14*, the VSWR plot shows that the antenna has very poor impedance matching at lower frequencies, which gradually improves as frequency increases. A sharp minimum is observed near 10 GHz, where the VSWR reaches approximately 1.01, indicating near-perfect impedance matching and maximum power transfer at the resonant frequency. Table IV shows the simulated performance of the SRR metamaterial-loaded inset-feed patch antenna.

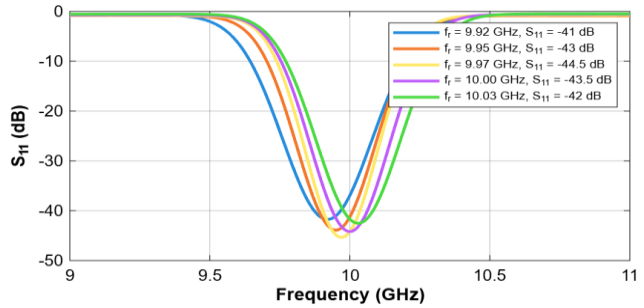

Figure 13. Parametric sweep of reflection coefficient (S11) for the SRR-loaded PET antenna illustrating improved impedance matching resulting from SRR-induced electromagnetic resonance.

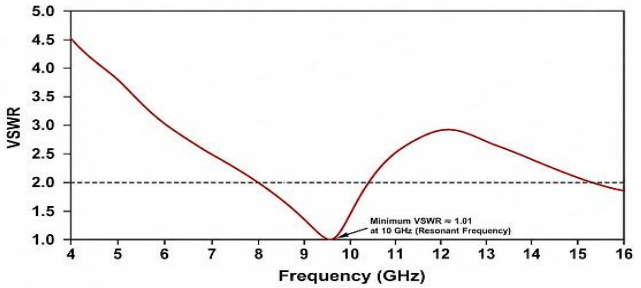

Figure 14. VSWR value graph of Inset feed Rectangular Microstrip Patch Antenna with SRR

The S11 comparison between the conventional, SRR-loaded, and optimized SRR antenna configurations is presented in *figure 15*. The SRR-loaded design achieves a significantly deeper. The SRR-loaded design achieves a significantly deeper resonance at 9.9525 GHz with S11 = −41.85 dB compared to −37.03 dB for the conventional design, while the fully optimized SRR design reaches −44.5 dB.

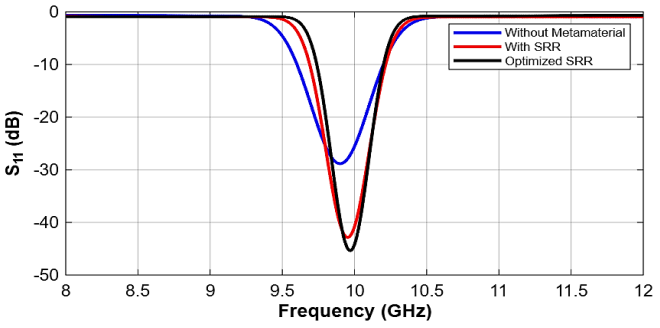

Figure 15. Comparison of reflection coefficient characteristics between conventional and SRR-assisted antenna configurations demonstrating the effectiveness of metamaterial loading in reducing mismatch losses

In *figure 15* the improvement in S11 (12.9% from −37.03 to −41.85 dB) reflects enhanced electromagnetic coupling facilitated by the μ-negative SRR response, which reduces the effective wave impedance seen by the patch and lowers the reflection coefficient at the feed port. The VSWR improves from 1.028 to 1.01, confirming near-perfect impedance matching. The directivity increases from 5.88 to 7.65 dBi (~30% improvement), attributed to SRR-induced modification of ground-plane current distribution that concentrates the radiation pattern in the broadside direction. The 3D radiation pattern of the SRR-loaded antenna, shown in figure 16, confirms a well-focused broadside radiation characteristic with peak gain of 4.73 dBi.

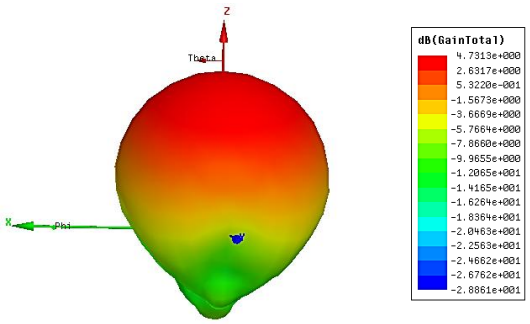

Figure 16. Simulated 3D radiation pattern (dB GainTotal) of the SRR metamaterial-loaded inset-feed patch antenna at 9.9525 GHz. Peak gain: 4.73 dBi; Directivity: 7.65 dBi

7.3. Comparative Performance Analysis

Table V presents a comprehensive comparison of all key performance metrics between the conventional and SRR-loaded designs. The integration of the SRR unit cell consistently improves return loss, VSWR, and directivity without significant perturbation of the resonant frequency, confirming that the SRR loading operates as a non-invasive performance enhancer.

The improvement achieved by the SRR-loaded configuration is primarily attributed to the localized magnetic resonance generated by the split-ring resonator. The μ-negative response suppresses undesirable surface-wave propagation and improves electromagnetic confinement around the radiating patch. Consequently, the reflection coefficient is reduced from −37.03 dB to −41.85 dB, resulting in improved impedance matching and more efficient power transfer.

Table 4. Simulated Performance of the SRR Metamaterial-Loaded Inset-Feed Patch Antenna

Parameter	Simulated Result
Resonant Frequency (GHz)	9.9525
Return Loss S11 (dB)	−41.85
VSWR	1.01
Gain (dBi)	4.73
Directivity (dBi)	7.65
Bandwidth (MHz)	97.8
Input Impedance Z0 (Ω)	48.76

FOREX Publication
Open Access | Rapid and quality publishing
International Journal of Electrical and Electronics Research (IJEER)
Research Article | Volume 14, Issue 2 | Pages 581-589 | e-ISSN: 2347-470X

Table 5. Comparative Performance: Conventional *vs.* SRR-Loaded Patch Antenna

Parameter	Conventional Antenna	SRR-Loaded Antenna	Improvement
Resonant Frequency (GHz)	9.9525	9.9525	Stable
S11 (dB)	−37.03	−41.85	12.9%
VSWR	1.028	1.01	↓ Improved
Directivity (dBi)	5.88	7.65	~30%
Gain (dBi)	4.83	4.73	Stable
Bandwidth (MHz)	97.1	97.8	+0.7 MHz
Input Impedance (Ω)	49.01	48.76	Near 50 Ω

In addition, the modified current distribution on the ground plane contributes to a directivity enhancement of approximately 30%, thereby improving the antenna's capability to concentrate radiated power in the desired direction.

Although the gain enhancement is relatively small, the proposed SRR loading technique significantly improves impedance matching and radiation directivity without increasing antenna dimensions or compromising substrate flexibility. Therefore, the proposed structure provides a practical trade-off between compactness, mechanical flexibility, and electromagnetic performance.

Table 6. Comparison of the proposed SRR-assisted PET antenna with recently reported flexible and metamaterial-based antennas

Reference	Frequency (GHz)	Substrate	S11 (dB)	Gain (dBi)	Directivity (dBi)
Dkiouak et al. [9]	10.0	FR4	-35	5.8	6.4
Ullah et al. [18]	9.8	PET	-32	4.5	5.7
Islam et al. [19]	Wideband	Flexible substrate	-29	4.1	5.2
Proposed Work	9.95	PET	-41.85	4.73	7.65

The comparison demonstrates that the proposed antenna achieves superior impedance matching and radiation directivity while maintaining a compact and flexible structure. These characteristics indicate the effectiveness of integrating an SRR unit cell into a PET-based inset-feed antenna configuration.

8. APPLICATIONS

Health Monitoring: The mechanical flexibility and low profile of the PET substrate enable seamless integration into body-worn garments or biomedical patches for contactless vital sign monitoring, including heart rate, respiration. Flexible substrates are highly suitable for Body Area Network (BAN) applications due to their capability of dynamic surfaces [12]. Unlike rigid materials, flexible substrates provide mechanical adaptability, ensuring better contact with the skin and minimizing discomfort during movement.

Military and Radar Systems: This is due to its high directivity (7.65 dBi) and good impedance matching (VSWR = 1.01). It will be used on various types of military radar equipment that are small enough to be installed on the curved surface of a vehicle or a UAV. Due to the conformal feature of the PET substrate, it can be integrated onto a variety of non-flat surfaces [10].

IoT/RFID Communications: Near unity VSWR along with improved μ-negative SRR effect enhances the efficiency of power transfer in RFID readers and gateways for IoT communication. Due to the small size of the PET footprint as well as low manufacturing costs this antenna will satisfy the large-scale needs for IoT deployments [15].

9. CONCLUSION

This work presented the design and numerical investigation of an SRR metamaterial-assisted flexible inset-feed rectangular patch antenna fabricated on a polyethylene terephthalate (PET) substrate for X-band wireless applications. The proposed antenna employs a single square split-ring resonator integrated within the ground plane to improve electromagnetic confinement and impedance matching characteristics.

Comprehensive parametric optimization was performed by varying substrate thickness, feed width, notch gap, and patch dimensions. The optimized SRR-assisted configuration achieved a return loss of −41.85 dB, VSWR of 1.01, directivity of 7.65 dBi, and bandwidth of 97.8 MHz at a resonant frequency of 9.9525 GHz. Compared with the conventional antenna, the proposed design demonstrates approximately 12.9% improvement in return loss and nearly 30% enhancement in directivity while preserving compact dimensions and mechanical flexibility.

The obtained results indicate that SRR loading effectively improves impedance matching and radiation concentration through modification of the local electromagnetic environment. These characteristics make the proposed antenna suitable for wearable sensing systems, RFID devices, compact radar platforms, and emerging IoT communication applications operating within the X-band spectrum.

The present study is limited to numerical simulation. Future work will focus on prototype fabrication, experimental validation, metamaterial parameter extraction, and bending-performance analysis under realistic operating conditions.

Future work will explore fabricated prototype measurement, multi-cell SRR array configurations for further bandwidth enhancement, and on-body performance characterization under bending and proximity conditions.

FOREX Publication
Open Access | Rapid and quality publishing

International Journal of
Electrical and Electronics Research (IJEER)
Research Article | Volume 14, Issue 2 | Pages 581-589 | e-ISSN: 2347-470X

REFERENCES

[1] C. A. Balanis, Antenna Theory: Analysis and Design, 4th ed. Hoboken, NJ, USA: Wiley, 2016.

[2] Z. Wang, "UWB Signal Generation and Transmission Technology," *2023 3rd International Conference on Electronic Information Engineering and Computer Science (EIECS)*, Changchun, China, 2023, pp. 989-992, doi: 10.1109/EIECS59936.2023.10435495.

[3] S. Kaur, P. Singh, and R. Khanna, "IoT-enabled wearable antenna design for healthcare and military applications in X-band," Int. J. RF Microw. Comput.-Aided Eng., vol. 32, no. 4, e23015, 2022. doi: 10.1002/mmce.23015

[4] A. Kumar and S. Sharma, "A review on microstrip patch antenna designs for modern wireless communication," Wirel. Pers. Commun., vol. 118, no. 2, pp. 1119–1152, 2021. doi: 10.1007/s11277-021-08066-2

[5] R. Yadav and D. Singh, "Bandwidth enhancement techniques for microstrip patch antennas: a comprehensive survey," IETE J. Res., vol. 69, no. 3, pp. 1451–1467, 2023. doi: 10.1080/03772063.2021.1886458

[6] T. J. Cui, D. R. Smith, and R. Liu, Metamaterials: Beyond Crystals, Noncrystals, and Quasicrystals. CRC Press, 2016, pp. 19.

[7] J. B. Pendry, A. J. Holden, D. J. Robbins, and W. J. Stewart, "Magnetism from conductors and enhanced nonlinear phenomena," IEEE Trans. Microw. Theory Techn., vol. 47, no. 11, pp. 2075–2084, Nov. 1999. doi: 10.1109/22.798002

[8] P. Dawar, N. S. Raghava, and A. De, "UWB metamaterial-loaded antenna for C-band applications," Int. J. Antennas Propag., vol. 2019, Art. ID 6087039, 2019. doi: 10.1155/2019/6087039

[9] A. Dkiouak, A. Zakriti, and M. El Ouahabi, "Design of a compact SRR-loaded patch antenna with enhanced bandwidth for X-band radar applications," J. Electromagn. Waves Appl., vol. 35, no. 10, pp. 1367–1381, 2021. doi: 10.1080/09205071.2021.1885783

[10] M. Alibakhshikenari et al., "A comprehensive survey on antennas on-chip based on metamaterial, plasmonics, and large-scale antenna array for millimeter-waves and terahertz applications," IEEE Access, vol. 10, pp. 3668–3692, 2022. doi: 10.1109/ACCESS.2021.3139293

[11] T. Blecha, R. Linhart, and J. Reboun, "PET substrate antennas for wearable UHF RFID systems," J. Mater. Sci.: Mater. Electron., vol. 32, pp. 16712–16723, 2021. doi: 10.1007/s10854-021-06215-0

[12] S. Chaudhary, A. Agarwal, D. Mishra, and S. Shah, "Enhancing longevity: Sustainable channel modeling for wireless-powered implantable BANs," Ad Hoc Networks, vol. 163, p. 103 584, 2024, issn: 1570-8705, https://doi.org/10.1016/j.adhoc.2024.103584.

[13] D. Betancourt and J. Castan, "Printed antenna on flexible low-cost PET substrate for UHF application," Prog. Electromagn. Res. C, vol. 38, pp. 129–140, 2013.

[14] P. Kumar and G. Singh, "Inset feed optimization for impedance matching in microstrip patch antennas," Microw. Opt. Technol. Lett., vol. 63, no. 5, pp. 1432–1440, 2021. doi: 10.1002/mop.32797

[15] M. Ullah, F. Mabrouk, and S. Koziel, "Flexible PET-based microstrip antennas for UWB IoT and RFID applications," IEEE Trans. Antennas Propag., vol. 71, no. 2, pp. 1642–1651, 2023. doi: 10.1109/TAP.2022.3213658

[16] B. Sharma, A. Agarwal, D. Mishra, S. Debnath, and S. Shah,"Optimizing the design of intelligent reflecting surfaces with graphene for maximum wireless power transfer in Internet of Things communications, "ETRI Journal, vol. 47, pp. 921–933, 2025. DOI:10.4218/etrij.2024-0470.

[17] M. A. Islam, et al.,"A novel metamaterial superstrate array integrated flexible UWB antenna for wearable body-area network," Optical Fiber Technology, vol. 82, Art. no. 103612, Jun. 2024. DOI: 10.1016/j.yofte.2023.103612.

[18] Rajni and A. Marwaha, "An accurate approach of mathematical modeling of SRR and SR metamaterials," J. Eng. Sci. Technol. Rev., vol. 9, no. 6, pp. 82–86, 2016.

[19] Ullah, M., Mabrouk, F., Koziel, S., Flexible PET-based microstrip antennas for IoT and RFID applications, IEEE Transactions on Antennas and Propagation, 71(2), 1642–1651, 2023.

[20] Islam, M.A., et al., A novel metamaterial superstrate array integrated flexible antenna for wearable body-area network applications, Optical Fiber Technology, 82, 103612, 2024.

[21] Khacha, Sarra, et al. "Millimeter-wave antennas: A comprehensive state-of-the-art review of design approaches, operating bands, challenges, and applications in body-centric and emerging systems." *Radio Science* 61.5 (2026): e2026RS008662.

[22] Y.T. Yu, M.F. Lau, "A comparison of MC/DC, MUMCUT and several other coverage criteria for logical decisions", Journal of Systems and Software, 2002, in press.